Integration of synchronised IR and PIV unsteady measurements on a channel flow

Integration of synchronised IR and PIV unsteady measurements on a channel flow

Journal of Physics: Conference Series **3173** (2026) 012018 doi:10.1088/1742-6596/3173/1/012018

Integration of synchronised IR and PIV unsteady measurements on a channel flow

A Cuéllar[1], E Amico[2], J Serpieri[2], G Cafiero[2], S Discetti[3], A Ianiro[3]

[1] Aerospace Systems and Transport Research Group, Universidad Rey Juan Carlos, Fuenlabrada, Spain
[2] Department of Mechanical and Aerospace Engineering, Politecnico di Torino, Torino, Italy
[3] Department of Aerospace Engineering, Universidad Carlos III de Madrid, Leganés, Spain

E-mail: antonio.cuellar@urjc.es

Abstract. Estimating velocity fields in wall-bounded turbulent flows using non-intrusive, wall-based measurements is a crucial challenge with significant implications for fundamental research and engineering applications like flow control. Traditional methods often rely on technically demanding intrusive probes or numerical simulations, which can be difficult to translate to real-world experimental setups. This study introduces a robust, non-intrusive experimental platform that uses infrared thermography with a heated thin-foil sensor to capture high-resolution, time-resolved measurements of unsteady heat transfer on a channel wall. These measurements are synchronized with particle image velocimetry data to enable the simultaneous acquisition of near-wall velocity fields. The methodology addresses key experimental challenges, including a low signal-to-noise ratio and the need for high-frequency acquisition. We demonstrate that the acquired heat transfer fluctuations show strong spatial and temporal coherence with near-wall structures, supporting their use for velocity field estimation. This work establishes a framework for generating reliable, synchronized datasets, paving the way for the development and validation of data-driven velocity field estimators and advanced active flow control strategies under realistic experimental conditions.

1 Introduction

1.1 Context and main objectives

Estimating flow velocity fields from wall-based data is a long-standing challenge in the study of wall-bounded turbulent flows. This task is motivated by its relevance to fundamental research [1]. Furthermore, it may be particularly relevant to engineering applications, such as the development of advanced flow control strategies in wall-bounded flows [2]. Traditionally, detailed information about turbulent structures within a channel has relied on either numerical simulations [3] or intrusive velocity measurements [4]—typically with a few probes—which can be costly and technically demanding in experimental settings.

Recent advances in data-driven techniques have demonstrated that it is possible to reconstruct or estimate near-wall velocity fields from signals obtained at the boundary, such as wall-shear stress, heat transfer, or pressure [5, 6]. Both linear (e.g., extended proper orthogonal decomposition, POD) [5], linear stochastic estimation [7]) and nonlinear techniques, including deep learning-based approaches (e.g., convolutional networks, generative adversarial networks)[8, 9], have been successfully deployed for this

purpose. Although promising results have been achieved using high-fidelity numerical data, translating these approaches successfully to experimental setups remains a crucial open step toward their practical implementation [10].

Implementing a flow sensing methodology based on non-intrusive sensors is essential in experimental environments to avoid introducing additional disturbances to the flow, preserving the flow dynamics of the boundary layer [11]. Otherwise, intrusive techniques can compromise measurement accuracy and the development of practical control systems. Such non-intrusive sensing strategies are a critical step towards creating viable prototypes for active flow control under realistic conditions.

In this context, a significant bottleneck is the acquisition of high-resolution, time-resolved measurements on the wall, along with the simultaneous recording of velocity fields in the near-wall region. Such data are necessary to train data-driven estimators capable of handling the complexities and inherent noise of real experiments. Each field comprises a large number of spatial points, resulting in a high-dimensional output space. This *curse of dimensionality* implies that the volume of training data required to achieve accurate estimation grows rapidly with the dimensionality of the output, which poses a significant obstacle in constructing reliable models from limited experimental or simulation data. Statistical learning theory formalises these difficulties, indicating that richer and more complex models require exponentially larger datasets to generalise well [12, 13]. The challenge is further compounded by the large number and dense spatial distribution of wall sensors required to capture the dynamics relevant to flow estimation and control [10].

This work introduces an experimental platform centered on the use of infrared (IR) thermography to capture high-resolution, time-resolved measurements of unsteady heat transfer directly at the wall in a turbulent channel flow. Leveraging a heated thin-foil sensor, this approach provides detailed spatial and temporal information about wall thermal dynamics, which are closely linked to near-wall turbulent structures. To enrich the analysis, these IR measurements are synchronized with particle image velocimetry (PIV) data, enabling the simultaneous acquisition of velocity fields. This integrated setup offers a powerful means to obtain paired wall and flow information under realistic experimental conditions, supporting advances in velocity field estimation.

Our primary objective is to develop a robust methodology based on high-resolution, time-resolved wall heat transfer measurements, which can be employed to generate reliable datasets and support the implementation and validation of velocity field estimators using wall observations. These models are specifically designed to handle the uncertainties, sensor noise, and environmental factors inherent to experimental conditions. Establishing this capability is a crucial step toward creating laboratory prototypes for active flow control systems grounded in real experimental data, ultimately enabling closed-loop control demonstrations in turbulent wall flows.

1.2 Heat transfer measurements: a strategic choice for wall-bounded flow diagnostics

This work aims to develop an experimental methodology for the synchronized acquisition of wall and fluid data in turbulent channel flows. Given the presence of coherent structures near the wall and the well-established correlations among various physical quantities in this region, these phenomena can be effectively studied using experimental data that simultaneously capture both wall and flow behaviour. Selecting which physical quantities to measure requires careful evaluation of available experimental techniques, aiming to identify optimal practices suited to the intended applications. Despite advances in measurement technology, it remains unfeasible to achieve high-resolution, two-dimensional sampling of multiple wall quantities simultaneously over surface areas comparable to those typically used in direct numerical simulations (DNS).

Among wall-based measurements, pressure fluctuations have been extensively studied due to their strong correlation with near-wall turbulence, both in experiments and simulations (e.g., [14, 4]). However, technological constraints limit the possibility of capturing unsteady wall pressure distributions with high spatial resolution over extended surfaces. The challenges arise from conflicting requirements on sensor size, sensitivity, and response time, which are difficult to satisfy simultaneously in turbulent flows with rapidly fluctuating signals. Wall-shear stress, another commonly studied quantity, can be experimentally quantified using techniques such as hot-film anemometry or oil-film interferometry [15]. Nevertheless, such techniques are intrusive or have limited spatial resolution and frequency response. Non-intrusive, wall-embedded shear stress sensors also face difficulties in detecting the typically low-amplitude fluctuations in turbulent channel flows and may lack the frequency response needed for unsteady measurements [16]. Consequently, acquiring high-resolution, time-resolved 2D measurements of wall pressure or shear stress remains a significant experimental challenge.

Heat transfer measurements offer a promising alternative that can overcome these limitations. The experimental approach adopted in this work, based on IR thermography and a heated thin foil embedded

in the wall—and therefore non-intrusive—enables high-frequency, high-resolution acquisition of unsteady convective heat transfer at the wall. The selection of heat transfer as the principal wall quantity is strongly supported by classical and contemporary research. The Reynolds analogy provides a theoretical foundation relating convective heat transfer and momentum transfer at the wall, though it holds strictly under idealized conditions such as constant fluid properties and simple flow regimes [17]. Importantly, seminal numerical studies have demonstrated strong spatial and temporal coherence between heat transfer fluctuations (thermal streaks) and wall-shear stress distributions, even beyond the strict applicability of the Reynolds analogy [18]. Furthermore, recent work [19] has successfully mapped wall-shear stresses to heat transfer fields in turbulent channel flows using convolutional neural networks, highlighting the complex nonlinear relationships that exist between these quantities.

These findings collectively support the viability of using experimentally measurable wall heat transfer as a surrogate to estimate velocity fields near the wall, opening new opportunities for experimental turbulence studies and active flow control strategies where direct measurement of wall shear or pressure at DNS-like resolution is not currently practical.

The heated-thin foil approach was pioneered in the context of wall-bounded flows, demonstrating its effectiveness for capturing wall heat transfer with high spatial and temporal resolution [20, 21]. More recently, this method was applied to a turbulent boundary layer in a water medium to perform unsteady heat transfer measurements [22], showcasing its adaptability across different fluids. However, heat transfer acquisition in the present experiment poses additional challenges due to the use of air as the working medium. Air's lower thermal diffusivity and density lead to significantly shorter characteristic times for near-wall thermal phenomena, requiring a high-frequency data acquisition system to accurately capture rapid fluctuations with low amplitude.

The expected heat transfer and temperature fluctuations in air have much lower amplitudes than in water, requiring sensors with higher sensitivity and signal-processing techniques to address the low signal-to-noise ratio. Tailored processing is also necessary because IR thermography—while non-intrusive and high-resolution—is inherently noisy due to electronic sensor noise, background radiation, and surface emissivity variations. Environmental disturbances like vibrations and airflow irregularities add further noise, complicating the reliable extraction of heat transfer signals. Thus, robust filtering, precise calibration, and careful data-cleaning procedures are required to achieve accurate, high-quality thermal measurements in air-based turbulent flow experiments.

Towards velocity estimation, an experimental dataset would be particularly valuable for training deep learning models via transfer learning, a method that uses a large synthetic dataset to pre-train a model before fine-tuning with a comparatively small amount of experimental data. However, the method may challenge the 'domain shift' between idealized simulations and real-world data, the need to create synthetic experimental data, the reduced correlation of wall heat flux compared to other wall quantities, and the threat of over-fitting due to the small size of the experimental dataset [23].

This work presents an overview of the experimental approach for measuring wall heat transfer in a turbulent channel, with full technical details of the sensor implementation available at [24]. It also covers its synchronization with PIV velocity measurements and analyzes the correlation between these mappings. The structure of this paper is as follows: Section 2 details the experimental setup, synchronization protocol, and data processing methods. Section 3 presents representative results from the heat transfer and combined measurements, a preliminary analysis of velocity estimation from wall data, and a discussion of the practical challenges encountered. Final remarks and prospects for future work are provided in Section 4. The experimental campaign related to this work has been conducted in the channel flow facility at Politecnico di Torino.

2 Methodology

This section contains a detailed description of the experimental setup and the established preprocessing procedure. Section 2.1 describes the IR instrumentation and setup, providing a justification for the different design choices. Further details on this topic can be found in a recent work by the coauthors [24]. Section 2.2 presents the details of the data processing. The experimental synchronization of the IR and PIV systems is discussed in section 2.3.

All experiments were conducted with the channel flow set at a friction-based Reynolds number $Re_\tau = 220$ with an Infratec Camera ImageIR® 6300Z. A diagram of the experimental setup is provided in Figure 1. The cross-section of the channel is 35×420 mm, extended for 10 m. The test section is a modular system that easily enables the integration of the different measurement techniques employed.

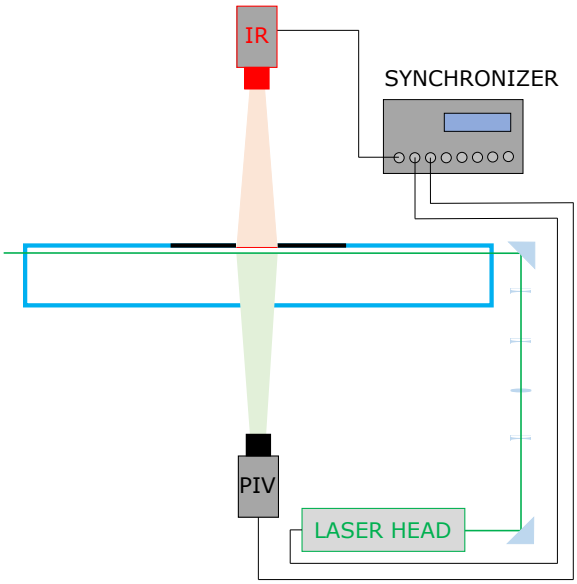

Figure 1: Cross-section of the experimental setup. The thin foil (red) and supporting frame (black) replace a section of the channel wall (blue). The IR camera records the external surface of the sensor. A system of mirrors and lenses generates a thin laser sheet parallel and close to the top wall of the channel. The PIV camera captures the illuminated region inside the channel, with the thin foil as background. A synchronizer provides the trigger signals for both the IR camera and the PIV system.

2.1 Experimental setup for IR thermography

The thin foil is mounted on a frame inserted into the channel structure, replacing one of its walls. The frame keeps the thin foil tight, flat, and aligned with the channel surface with minimal intrusiveness, discharges the current through it, and enables optical access to the foil surface from the external side of the channel. The thin foil is made of a CrNi-steel alloy with a high resistivity. Electric current is discharged through the foil so that it is heated by the Joule effect, assuming a constant and uniform heat flux distribution. Uniform material properties and symmetric copper–indium contacts promote a spatially homogeneous current, while the measured temperature field confirmed the absence of localized heating, supporting the validity of this assumption. The local energy balance (1) is employed to compute the heat transfer coefficient h_c. It considers heat flux effects due to the input power heating the foil ϕ''_{J}, conduction through the foil ϕ''_{cond}, radiation on both surfaces ϕ''_{rad}, and convection on the internal $h_c(T_{\mathrm{w}} - T_{\mathrm{aw}})$ and external sides $\phi''_{\mathrm{conv,ext}}$. These heat fluxes can be computed in terms of the foil thickness a, its thermal and mechanical properties, such as density ρ, heat capacity c_p, thermal conductivity κ, or emissivity ϵ, and the temperature 2D mappings from the IR camera.

$$c_p \rho a \frac{\partial T_{\mathrm{w}}}{\partial t} = \phi''_{\mathrm{J}} - \phi''_{\mathrm{cond}} - 2\phi''_{\mathrm{rad}} - \phi''_{\mathrm{conv,ext}} - h_c(T_{\mathrm{w}} - T_{\mathrm{aw}}) \ , \tag{1}$$

where T_{w} is the local temperature on the wall surface and T_{aw} is the adiabatic temperature. The constraints to perform this high-frequency heat transfer sensing system were introduced in section 1.2. These limitations and assumptions bring a set of technical and operational requirements. The small amplitude of the fluctuations, together with the low signal-to-noise ratio of the IR acquisition, requires a certain level of heating. Meanwhile, excessive heating may perturb the flow, creating buoyancy effects, increasing the Richardson number. Inside the channel, forced convection must therefore dominate over natural convection ($Ri \ll 0.1$). Despite the signal amplification, the thermal resolution of the camera must be small enough to capture the small temperature changes.

The setup relies on the thermally thin-foil assumption. The field of view of the camera intercepts the external surface of the foil, reading temperature maps considered representative of the internal surface. This requires a Biot number $Bi \ll 1$ for the assumption to hold, which restricts the thickness of the foil to the micro-scale—foils of 5 and 10 μm were employed. The frame and copper blocks keep the thin foil in tension during operation and minimize flow-induced motion, motivating the choice of a high-tensile strength steel alloy. No visible vibrations or temperature fluctuations associated with mechanical oscillations were detected at the operating Reynolds number. While micro-vibrations cannot be entirely

ruled out, they are expected to have a negligible influence on the large-scale flow and heat-transfer measurements considered in this study.

The foil, even if thin, introduces a certain thermal inertia in the problem, delaying heat transfer. Its characteristic time—related to the delay—must remain negligible compared to the convective timescale. This can be evaluated with the Fourier number, which must be $Fo \gg 1$ [25]. Furthermore, a high-frequency acquisition system is also needed to properly capture flow unsteadiness, providing enough sampling of each event. Sufficiently large temporal resolution is indeed needed to reduce the uncertainty from the unsteady term in equation (1).

Additionally, the thin foil has been coated with a black matte, high-emissivity paint on both sides. On the external side, it enhances the quality of IR measurements in conditions with very small temperature fluctuations. On the internal side, it provides a suitable black matte background for PIV measurements (setup and synchronization are described below in section 2.3). The unsteady term and the conductive heat flux in (1) were adjusted to include the paint's thermal properties.

The experimental setup was designed considering these requirements, under the operational conditions of the channel airflow and the capabilities of the instrumentation. The IR camera operated at 180 Hz, as a compromise between temporal and spatial resolution. This ensures that each eddy turnover time is sampled 16 times, while the field of view covers the entire sensor with a spatial resolution of about 5 px/mm.

2.2 Data processing methods

A filtering scheme was needed to enhance the quality of temperature maps and isolate the contribution of the coherent structures within the channel fluid dynamics.

Visualization of the sequence first revealed low-frequency oscillations, with a characteristic size comparable to the sensor surface, coexisting with other smaller-scale, high-frequency phenomena. Although the Richardson number ensures that forced convection dominates inside the channel, natural convection cells developed on the top external side of the foil. To remove this effect, a high-pass filter with a cutoff frequency of 0.9 Hz was applied. This eliminates the low-frequency content while preserving the channel flow dynamics, with more than one order of magnitude of margin to reach the characteristic eddy turnover time. The choice of this filter, rather than a narrow-band filter centered on the natural convection frequency, has the additional advantage of removing other low-frequency or constant reflections not representative of channel turbulence. In consistency with equation (1), the external convective term was therefore neglected once this filter was applied.

A 3D-Gaussian filter was then applied. With a kernel size of 2 pixels in both spatial directions, this filter reduced noise associated with pixel-scale fluctuations. In addition, a POD-based filter removed the low energetic and noisy modes, with the cutoff mode determined using the elbow method.

These filters substantially reduced the noise level and revealed patterns consistent with the footprint of the coherent structures on the channel. However, an additional 3D-Gaussian filter with a rectangular kernel was employed to suppress striped patterns associated with the IR camera acquisition mechanism. The resulting filtered images were employed to compute h_c from equation (1). In its dimensionless form, Stanton number $St = \frac{h_c}{\rho U_\infty c_p}$ maps show patterns with characteristic scales consistent with this type of channel flow [26]. The average autocorrelation map was calculated to uncover the typical size and shape of patterns that appear in the flow (see Figure 2). A single autocorrelation map shows the similarities of a pattern when it is shifted in different directions. When they are averaged together, random noise cancels out, and relevant patterns stand out. The map is normalized by the variance of the data. This reveals streamwise-aligned patterns with average sizes that are statistically consistent with those visually observed in the instantaneous samples.

2.3 Synchronization protocol

The experimental setup for IR data acquisition was combined with planar PIV to measure the flow field, as shown in the sketch in Figure 1. To this end, an Andor Zyla 5.5 camera and a Litron Nano L 200-15 PIV laser with an LPU550 power supply were used. The camera has a resolution of 2560 × 2160 and a pixel size of 6.5μm, and is equipped with a lens with a focal length of 60 mm. The laser emits 532 nm green light with an energy of up to 200 mJ per pulse, and the pulse pair is separated by a 180 μs time interval. The flow is seeded with DEHS (Di(2-ethylhexyl)sebacate) particles with a 1.2 μm diameter for PIV purposes. The laser beam is converted into a thin, uniform laser sheet using a combination of cylindrical divergent and spherical convergent/divergent lenses. This sheet is then positioned parallel to and near the channel wall by two mirrors, at a distance of about $y^+ \approx 30$ for the experiments presented in this work.

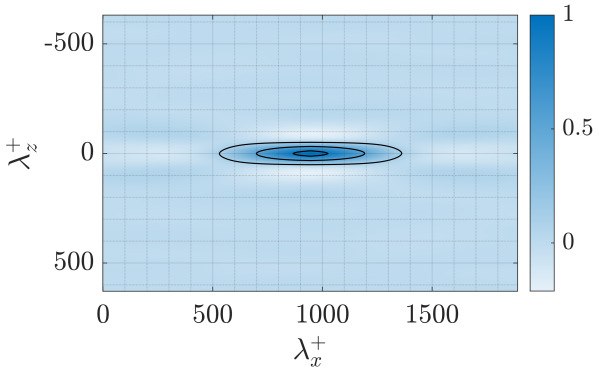

Figure 2: Average 2D autocorrelation map of St fluctuations, highlighting the characteristic size and orientation of the coherent flow structures in the dataset. Contoured isolines correspond to the levels 0.1, 0.5, and 0.9 of the autocorrelation value.

Regarding the PIV setting and processing, each image pair was acquired with a time interval of 180 μs. The original images were pre-processed using a POD-based background removal algorithm [27] before being used for PIV processing. The processing was carried out with a multi-grid image deformation method [28], implemented in the software PaIRS of the University of Naples [29]. It was configured iteratively, beginning with a 64 × 64 window size, followed by two additional iterations with a 48 × 48 window, all with a window overlapping parameter of 0.75. Velocities are obtained on a mesh with spacing $\Delta x^+ \approx \Delta z^+ = 8.6$.

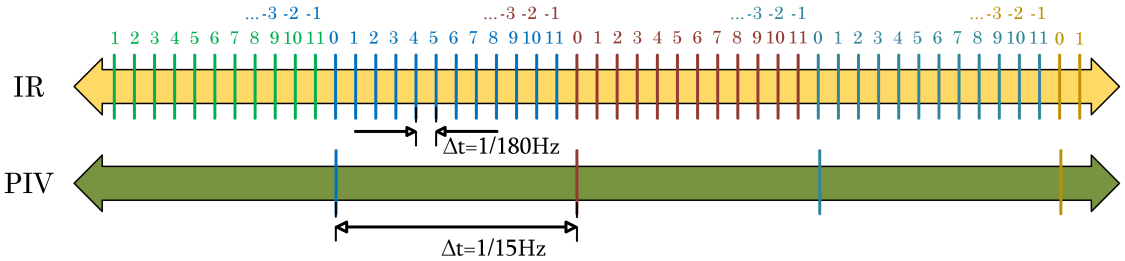

Figure 3: A time diagram of the trigger signals for the IR and PIV systems. A PIV pulse is coincident with an IR pulse (pulse 0). In each 15 Hz cycle, 11 additional IR pulses occur at intervals of $\Delta t = \frac{1}{180\text{Hz}}$ before the next coincidence with the PIV system.

The synchronizer sets the trigger signals for the laser heads and the PIV camera. The choice of two different frequencies for the systems was made to accommodate the specific constraints of each measurement. The PIV system operates at a sampling frequency of 15 Hz, a limit imposed by the laser heads. The time step between consecutive velocity samples (0.0666 s) is shorter than the eddy turnover time (0.0894 s). Conversely, the IR acquisition frequency was set to 180 Hz to provide sufficient temporal resolution for computing the time derivatives required for heat transfer calculations, which would be unfeasible at 15 Hz. This frequency was chosen as a multiple of the PIV sampling frequency (180 Hz = 12 x 15 Hz) to enable direct comparison of the two datasets. In this way, 12 phased IR samples are obtained for each PIV image pair, with one sample synchronized with the PIV trigger, and the other 11 pulses are sequentially emitted each $\Delta t = 1/180$ s until the next PIV trigger. This condition offers the advantage of obtaining a dataset with both phase-delayed and phase-advanced IR-PIV mapping pairs, rather than just instantaneous pairs. This synchronization is depicted in Figure 3.

3 Results

3.1 Heat transfer measurements

This section summarizes the key findings from Ref. [24], specifically addressing the effects of heating and foil thickness on the infrared (IR) measurements.

The first key finding relates to the effect of heating. A certain level of heating is necessary to amplify the thermal signal, which facilitates IR acquisition of the thermal footprint on the channel wall. Different heating levels—corresponding to Joule power inputs that raise the average temperature 15, 25, and 35 K above room temperature—were tested. Higher heating levels result in a greater variance in the filtered temperature maps and lower noise. Consequently, the 35 K heating level was identified as the optimal case, as it provides the most physically consistent heat transfer fluctuation maps.

The effect of foil thickness was also analysed. A thicker foil—with extra mass—introduces additional thermal inertia, even while the thin-foil assumption remains valid. According to the energy balance equation, this impacts the unsteady and conduction terms, affecting the response times. To assess this, the 5 μm foil was replaced with a 10 μm foil. Changes in the thermal streaks were observed to be slower, with slightly attenuated peaks and variance. Additionally, the sequence obtained with the thicker foil was noisier. However, the observed patterns maintained similar sizes and shapes, which denotes coherence with the channel flow dynamics and validates the methodology. Given these findings, the thinner 5 μm foil is the preferred option when possible, as it reduces noise and better aligns with the $Bi \ll 1$ and $Fo \gg 1$ assumptions.

Considering these results, the most suitable configuration for obtaining clear and physically consistent data is the 5 μm foil heated to approximately 35 K above room temperature. This choice is supported by the uncertainty quantification analysis, as this specific configuration was the only one to yield an uncertainty below 10%. The analysis, performed using a Monte Carlo approach with a 99% confidence interval on a Gaussian distribution, revealed that uncertainty primarily increases with a reduction in Joule power. The effect of foil thickness on uncertainty is less pronounced, as the increased contribution from the temporal derivatives is offset by a relatively lower contribution from other variables.

3.2 Combined measurements

Some points at the borders of the sensor have been identified on the heat transfer and velocity mappings to ensure alignment and spatial correspondence between both datasets. To ensure the correspondence between both measured quantities, the average 2D correlation map of the heat transfer fluctuation ΔSt and the streamwise velocity fluctuation map $\Delta u'$ has been computed. To that end, instantaneous—same trigger signal—2D mappings have been considered. This procedure was repeated for the different samples on a dataset with 30,000 PIV samples, and the instantaneous correlation maps were averaged and normalised, providing a different view of the near-wall coherent structures and their thermal footprint in Figure 4. Even though the correlation is not straightforward, with peaks of the order of 0.2, it shows their presence and depicts their characteristic shape.

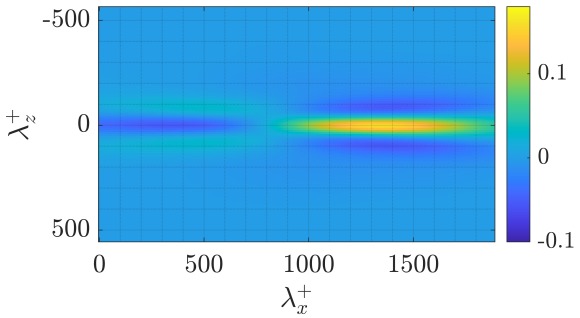

Figure 4: Average 2D correlation map of $\Delta u'$ and ΔSt over a sequence with 30,000 samples with instantaneous trigger signal for the PIV and IR acquisition systems.

The difference in the sampling frequencies of both systems enables an assessment of this correlation with phased pairs, rather than just with the instantaneous pair. Taking into account different phase conditions, Figure 5 shows how this highly correlated region progressively shifts as a consequence of flow advection. As observed in Figure 2, regions with a negative correlation coefficient are reported on both sides in the spanwise direction, and also upstream and downstream. The moderate correlation levels are consistent with the non-linear relationship between heat transfer and velocity, as well as the experimental noise and spatial averaging inherent to the IR measurements.

The purpose of this experimental setup was to develop a flow-sensing approach to obtain a database of synchronized samples of the flow field and wall data, for applications such as studying instantaneous flow estimation. This phasing situation brings the opportunity to additionally address this flow estimation from time-delayed or time-advanced wall data. For example, towards the development of a flow control

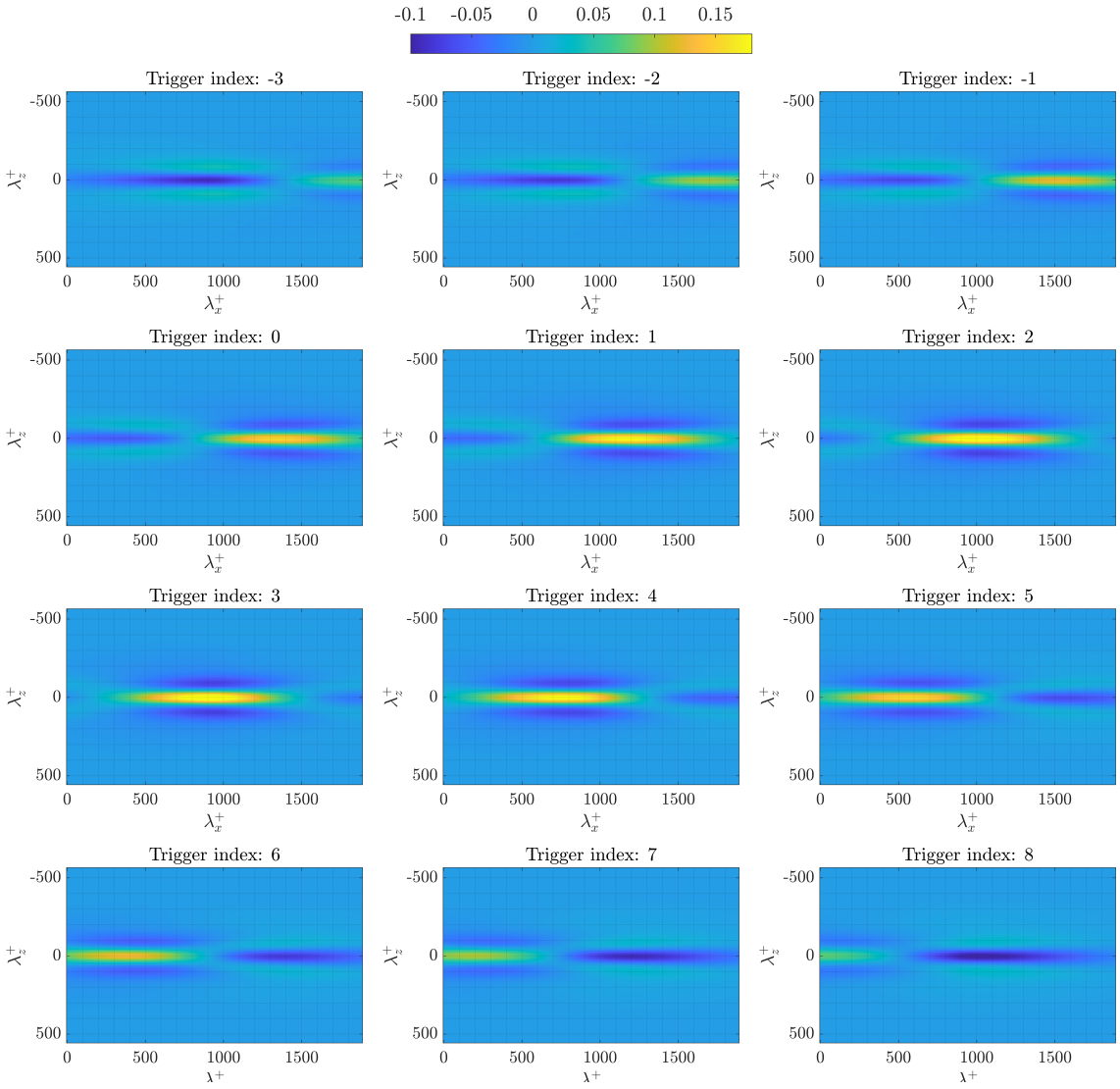

Figure 5: Sequence of average 2D correlation map of $\Delta u'$ and ΔSt over a sequence with 30,000 samples, for phased trigger signals at 180 Hz of the IR system.

algorithm, it could be interesting to estimate the flow field downstream based on the wall information sensed a few instants of time before, providing us with a prediction of the flow behaviour, facilitating the actuation on large-scale features downstream. Figure 2 anticipates that the quality of the correlation and the location of the correlated region depend on the timing.

4 Discussion, practical challenges & future work

This experimental setup provides a powerful framework for developing and validating flow estimation models that use real-world data rather than purely simulations. The ability to acquire time-resolved, synchronized, and phased samples of both wall heat transfer and near-wall velocity fields allows researchers to explore new estimation strategies. For instance, a key potential application is the development of feedback-feedforward control algorithms. By using wall information sensed at a specific moment to predict the downstream flow field, it could be possible to feed a controller to modify large-scale flow features. This capability is vital for creating effective closed-loop control systems. While challenges remain, such as accommodating the inherent noise and sensor resolution differences due to the 'domain shift', the platform's robust data acquisition and processing procedures provide a solid foundation for tackling these issues.

The implementation of this experimental platform encountered several practical challenges. Firstly,

the use of air as the working medium posed a significant hurdle due to its low thermal diffusivity and density. This resulted in low-amplitude heat transfer and temperature fluctuations, requiring a highly sensitive sensor and specialized signal-processing techniques to address the low signal-to-noise ratio. To overcome this, the system required a certain level of heating to amplify the thermal signal, while simultaneously ensuring that the heating did not induce buoyancy effects that could perturb the flow. Secondly, two different measurement systems (IR and PIV) with distinct sampling frequencies were synchronised. The IR frequency was set as a multiple of the PIV frequency, allowing for direct comparison and analysis of both instantaneous and phased datasets. Lastly, IR thermography is inherently noisy due to electronic sensor noise, background radiation, and surface emissivity variations, which necessitated the development of a tailored filtering scheme, including high-pass and Gaussian filters, to isolate the relevant flow dynamics from environmental disturbances.

This study successfully developed and validated an experimental platform that provides a robust framework for flow estimation and control. A strong spatial and temporal coherence between wall heat transfer and near-wall velocity fluctuations was observed, demonstrating that heat transfer can be a viable surrogate for velocity estimation in an experimental setting. The ability to acquire time-phased data, enabled by a precise synchronization protocol, might be an interesting contribution to the development of predictive models.

Future efforts will focus on several key areas to build upon this foundation. Firstly, the tuning and optimization of the experimental setup will continue, with the aim of further improving the signal-to-noise ratio and extending the capabilities of the measurement system. This includes studying the impact of alternative filter configurations. Secondly, the generated dataset of synchronized IR and PIV measurements will be used to develop and validate advanced inference algorithms, such as machine learning models, for velocity field estimation. The phased data pairs are particularly valuable for training models that can perform time-delayed or time-advanced predictions, a key requirement for effective flow control. Finally, the ultimate goal is to integrate the sensing platform with flow actuators to demonstrate active closed-loop control in a turbulent flow environment. This would provide a real-world, laboratory-scale prototype for active flow control systems that are grounded in experimental data.

Acknowledgements A.C. acknowledges financial support from the Spanish Ministry of Universities under the FPU programme 2020. This activity is part of the project EXCALIBUR (Grant No PID2022-138314NB-I00), funded by MCIU/AEI/10.13039/501100011033 and by "ERDF A way of making Europe".

References

[1] I Marusic, B J McKeon, P A Monkewitz, H M Nagib, A J Smits, and K R Sreenivasan. Wall-bounded turbulent flows at high reynolds numbers: recent advances and key issues. *Phys Fluids*, 22(6), 2010.

[2] A Cremades, S Hoyas, R Deshpande, P Quintero, M Lellep, W J Lee, J P Monty, N Hutchins, M Linkmann, I Marusic, et al. Identifying regions of importance in wall-bounded turbulence through explainable deep learning. *Nat Commun*, 15(1):3864, 2024.

[3] C Chen and L He. On locally embedded two-scale solution for wall-bounded turbulent flows. *J Fluid Mech*, 933:A47, 2022.

[4] D J C Dennis and T B Nickels. Coherent structures in wall-bounded turbulence. *Annu Rev Fluid Mech*, 47:165–184, 2015.

[5] A Güemes, S Discetti, and A Ianiro. Sensing the turbulent large-scale motions with their wall signature. *Phys Fluids*, 31(12), 2019.

[6] F R Amaral, A VG Cavalieri, E Martini, P Jordan, and A Towne. Resolvent-based estimation of turbulent channel flow using wall measurements. *J Fluid Mech*, 927:A17, 2021.

[7] M P Encinar and J Jiménez. Logarithmic-layer turbulence: a view from the wall. *Phys Rev Fluids*, 4(11):114603, 2019.

[8] A Güemes, S Discetti, A Ianiro, B Sirmacek, H Azizpour, and R Vinuesa. From coarse wall measurements to turbulent velocity fields through deep learning. *Phys Fluids*, 33(7), 2021.

[9] A Cuéllar, A Güemes, A Ianiro, Ó Flores, R Vinuesa, and S Discetti. Three-dimensional generative adversarial networks for turbulent flow estimation from wall measurements. *J Fluid Mech*, 991:A1, 2024.

[10] A Cuéllar, A Ianiro, and S Discetti. Some effects of limited wall-sensor availability on flow estimation with 3D-GANs. *Theor Comp Fluid Dyn*, 38(5):729–745, 2024.

[11] S Pasch, R Leister, D Gatti, R Örlü, B Frohnapfel, and J Kriegseis. Measurements in a Turbulent Channel Flow by means of an LDV Profile Sensor. *Flow Turbul Combust*, 113(1):195–213, 2024.

[12] C M Bishop and N M Nasrabadi. *Pattern recognition and machine learning*, volume 4. Springer, 2006.

[13] T Hastie, R Tibshirani, J Friedman, et al. The elements of statistical learning, 2009.

[14] W J Baars, N Hutchins, and I Marusic. Self-similarity of wall-attached turbulence in boundary layers. *J Fluid Mech*, 823:R2, 2017.

[15] R Örlü and P Schlatter. Comment on "Evolution of wall shear stress with Reynolds number in fully developed turbulent channel flow experiments". *Phys Rev Fluids*, 5(12):127601, 2020.

[16] O Amili and J Soria. A film-based wall shear stress sensor for wall-bounded turbulent flows. *Exp Fluids*, 51(1):137–147, 2011.

[17] H Schlichting and K Gersten. *Boundary-layer theory*. Springer, 2016.

[18] H Abe and R A Antonia. Near-wall similarity between velocity and scalar fluctuations in a turbulent channel flow. *Phys Fluids*, 21(2), 2009.

[19] J Kim and C Lee. Prediction of turbulent heat transfer using convolutional neural networks. *J Fluid Mech*, 882:A18, 2020.

[20] H Nakamura. Frequency response and spatial resolution of a thin foil for heat transfer measurements using infrared thermography. *Int J Heat Mass Tran*, 52(21-22):5040–5045, 2009.

[21] H Nakamura and S Yamada. Quantitative evaluation of spatio-temporal heat transfer to a turbulent air flow using a heated thin-foil. *Int J Heat Mass Tran*, 64:892–902, 2013.

[22] F Foroozan, A Güemes, M Raiola, R Castellanos, S Discetti, and A Ianiro. Synchronized measurement of instantaneous convective heat flux and velocity fields in wall-bounded flows. *Meas Sci Technol*, 34(12):125301, 2023.

[23] L Guastoni, A G Balasubramanian, F Foroozan, A Güemes, A Ianiro, S Discetti, P Schlatter, H Azizpour, and R Vinuesa. Fully convolutional networks for velocity-field predictions based on the wall heat flux in turbulent boundary layers. *Theor Comp Fluid Dyn*, 39(1):13, 2025.

[24] A Cuéllar, E Amico, J Serpieri, G Cafiero, W J Baars, S Discetti, and A Ianiro. Measuring time-resolved heat transfer fluctuations on a heated-thin foil in a turbulent channel airflow. *Meas Sci Technol*, 36(4):045303, 2025.

[25] T Astarita and G M Carlomagno. *Infrared thermography for thermo-fluid-dynamics*. Springer, Berlin, Heidelberg, 2013.

[26] J C Del Álamo and J Jiménez. Spectra of the very large anisotropic scales in turbulent channels. *Phys Fluids*, 15(6):L41–L44, 2025.

[27] M A Méndez, M Raiola, A Masullo, S Discetti, A Ianiro, R Theunissen, and J-M Buchlin. Pod-based background removal for particle image velocimetry. *Experimental Thermal and Fluid Science*, 80:181–192, 2017.

[28] F Scarano. Iterativeimage deformation methods in piv. *Meas Sci Technol*, 13(1):R1, 2002.

[29] G Paolillo and T Astarita. PaIRS-UniNa: A robust and accurate free tool for digital particle image velocimetry and optical camera calibration. In *Proceedings of 21st International Symposium on Applications of Laser and Imaging Techniques to Fluid Mechanics*, Lisbon, Portugal, July 08–11 2024.